#### **Research Article**

Mohamed S. Nafie<sup>#</sup>, Nada K. Sedky<sup>#</sup>, Hatem A. F. M. Hassan, Iten M. Fawzy, Manal M. M. Abdelhady, Udo Bakowsky\*, and Sherif Ashraf Fahmy\*

# PEG-PLGA core-shell nanoparticles for the controlled delivery of picoplatin-hydroxypropyl β-cyclodextrin inclusion complex in triplenegative breast cancer: *In vitro* and *in vivo* study

https://doi.org/10.1515/ntrev-2024-0115 received March 16, 2024; accepted October 14, 2024

**Abstract:** In this study, we prepared an inclusion complex of picoplatin (Pc) with 2-hydroxy propyl β cyclodextrin (HPCD) to improve its hydrophilicity, yielding Pc-HPCD. The Pc-HPCD complex was encapsulated into PEG-PLGA nanoparticles (NPs) using the emulsion–solvent evaporation method, yielding Pc-HPCD@PEG-PLGA core–shell NPs. The inclusion complex was assessed using <sup>1</sup>HNMR spectroscopy and a phase solubility study. In addition, the average hydrodynamic diameter, polydispersity index, zeta potential,

# These authors contributed equally to this work and should be considered first co-authors.

**Iten M. Fawzy:** Department of Pharmaceutical Chemistry, Faculty of Pharmacy, Future University in Egypt, 11835, Cairo, Egypt **Manal M. M. Abdelhady:** Clinical Pharmacy Department, Faculty of Pharmacy, Badr University, Cairo, 11829, Egypt

and encapsulation efficiency (EE%) of the Pc-HPCD@PEG-PLGA NPs were 190.2  $\pm$  8.7 nm, 0.14  $\pm$  0.02,  $-13.97 \pm$  0.67 mV, and 80.7 ± 2.4%, respectively. In vitro release study showed a pH-triggered release manner. Furthermore, the biological evaluation of Pc-HPCD@PEG-PLGA NPs revealed a significantly potent cytotoxic activity (IC<sub>50</sub> =  $1.6 \pm 0.24 \mu g/ml$ ) against triple-negative breast cancer cells (TNBC), surpassing that of Pc-HPCD (IC<sub>50</sub> =  $5.3 \pm 0.93 \,\mu\text{g/ml}$ ) and Pc (IC<sub>50</sub> =  $7.5 \pm 0.4 \,\mu\text{g/ml}$ ). Pc-HPCD@PEG-PLGA NPs induced significant apoptosis and the ability to arrest cells at the sub-G1 phase in MDA-MB-231 cells. Moreover, in an in vivo model established using SECbearing mice, treatment with Pc-HPCD@PEG-PLGA demonstrated significant inhibition of tumor proliferation (67.2%). This was accompanied by improvements in hematological and biochemical measurements, as well as histopathological examination, which indicated a reduction in cellular and nuclear pleomorphism. Our study demonstrated the potential of Pc-HPCD@PEG-PLGA NPs to be employed as an effective and safe therapy capable of conquering TNBC.

**Keywords:** picoplatin, hydroxypropyl-β-cyclodextrin, inclusion complex, PEG-PLGA nanoparticles, cytotoxicity, apoptosis, cell cycle arrest, triple-negative breast cancer (MDA-MB-231)

#### 1 Introduction

Cancer is one of the major health burdens all over the world, with millions of new cases each year [1]. Breast cancer is one of the most prevalent types of cancer worldwide. It is categorized into either ERBB2-positive breast cancer, hormone receptor-positive breast cancer, or triplenegative breast cancer (TNBC). Unlike the first two types, TNBC is extremely hostile and highly resistant to most current chemotherapeutics. Thus, a combinatorial therapy is required to achieve the desired anticancer effects. However, the use of combinatorial chemotherapy is accompanied by

<sup>\*</sup> Corresponding author: Udo Bakowsky, Department of Pharmaceutics and Biopharmaceutics, University of Marburg, Robert-Koch-Str. 4, 35037, Marburg, Germany, e-mail: ubakowsky@aol.com, tel: +49-(0)-6421-28-2-58-84

<sup>\*</sup> Corresponding author: Sherif Ashraf Fahmy, Department of Pharmaceutics and Biopharmaceutics, University of Marburg, Robert-Koch-Str. 4, 35037, Marburg, Germany; Department of Chemistry, School of Life and Medical Sciences, University of Hertfordshire Hosted by Global Academic Foundation, R5 New Garden City, New Capital, Cairo, 11835, Egypt, e-mail: sheriffahmy@aucegypt.edu, tel: +20 1222613344 Mohamed S. Nafie: Department of Chemistry, College of Sciences, University of Sharjah, Sharjah, P.O. 27272, United Arab Emirates Nada K. Sedky: Department of Biochemistry, School of Life and Medical Sciences, University of Hertfordshire Hosted by Global Academic Foundation, R5 New Garden City, New Administrative Capital, Cairo, 11835, Egypt Hatem A. F. M. Hassan: Medway School of Pharmacy, University of Kent, Chatham Maritime, Kent, ME4 4TB, United Kingdom; Department of Pharmaceutics and Industrial Pharmacy, Faculty of Pharmacy, Cairo University, 11562, Cairo, Egypt

severe systemic side effects. Thus, the discovery of effective preferential therapy against TNBC with minimum toxicity in healthy cells is required [2]. Platinum-based chemotherapeutic drugs (PBDs), such as cisplatin and carboplatin, are potent antitumor treatments synthesized through the coordination complexation of platinum (Pt) [3]. These drugs are widely utilized and are effective against various solid tumors, including breast cancer. Since the FDA approval of cisplatin (Scheme 1a), the first-generation PBD, in 1979, a multitude of platinum complexes have been developed [3-5]. Examples include satraplatin, carboplatin, nedaplatin, and oxaliplatin. Despite the extensive development, only ten compounds have undergone clinical trials, exploring their potential applications in cancer therapy. Among these synthesized compounds, the Pt(II) complex, picoplatin (Pc, Scheme 1b), has been developed to address certain drawbacks associated with cisplatin, such as intrinsic chemoresistance and intolerable toxic side effects. In addition, Pc has demonstrated a broad and potent anticancer effect against various types of tumor cells [6]. More importantly, Pc showed considerable cytotoxicity against the most aggressive and resistant type of breast cancer, triplenegative breast cancer (TNBC), as compared to cisplatin.

The enhanced actions of Pc compared to cisplatin are attributed to the presence of the 2-methylpyridine group. This group serves as a steric bulk, impeding the axial approach of nucleophiles to the platinum center without diminishing the level of DNA platination [7].

Nonetheless, the clinical translation of Pc in cancer therapy is significantly constrained by its hydrophobic nature and poor biodistribution profiles. While this study primarily focused on improving the hydrophilicity of Pc through the inclusion complex formation with 2-hydroxy propyl  $\beta$  cyclodextrin (HPCD), further investigation is needed to explore bioavailability enhancement approaches, including alternative administration routes [6].

Cyclodextrins (CDs) and their derivatives are amphiphilic cyclic oligosaccharides with a hydrophobic core and

Scheme 1: Chemical structures of (a) cisplatin, (b) Pc, and (c) PEG-PLGA.

a hydrophilic external surface. Among these derivatives, HPCD plays a crucial role in overcoming the poor aqueous solubility of various-sized hydrophobic guest molecules by forming host-guest inclusion complexes. This could be attributed to its hydrophilicity and capability to form water-soluble inclusion complexes with various hydrophobic therapeutic agents [8,9]. Besides, the demonstrated biocompatibility of HPCD has promoted its utilization in enhancing the aqueous solubility of hydrophobic drugs. In addition, various strategies have been developed to improve the controlled release and targeting ability of different drugs to malignant cells. In this context, the nanoencapsulation of inclusion complexes into polymeric nanoparticles (NPs) represents a promising approach for fabricating smart drug delivery systems. Poly(ethylene glycol) methyl ether-block-poly (lactide-co-glycolide) (PEG-PLGA) is a diblock amphiphilic copolymer (Scheme 1c) capable of encapsulating various drugs via self-assembly in an aqueous medium, forming core-shell nanoemulsions [10]. Additionally, PLGA and PEG have received FDA approval owing to their biocompatibility and biodegradability [11,12].

To this end, we synthesized the Pc-HPCD inclusion complex to increase Pc's aqueous solubility. To offer a controlled release profile and tumor targeting ability, the designed complex was encapsulated into PEG-PLGA NPs, forming Pc-HPCD@PEG-PLGA NPs with a core-shell structure utilizing the modified double-emulsion solvent-evaporation method (W/O/W). The engineered NPs were then evaluated for size, zeta potential, polydispersity index (PDI), encapsulation efficiency (EE%), morphology, and release manner. In addition, the cytotoxic activity of Pc-HPCD@PEG-PLGA NPs, Pc-HPCD, and Pc was evaluated against triple negative (MDA-MB-231) breast cancer and the healthy breast epithelial (MCF10A) cells. The HPCD@PEG-PLGA NPs underwent further flow cytometric detection for apoptosis and cell cycle analysis. To the best of our knowledge, no previous studies have reported the nanoformulation of the Pc-HPCD inclusion complex into core-shell PEG-PLGA NPs to improve its toxicity against TNBC.

#### 2 Materials and methods

#### 2.1 Materials

Pc and HPCD were bought from Abcam, Germany. Poly (ethylene glycol) methyl ether-block-poly (lactide-co-glycolide) with PEG (average molecular weight of 2,000 g/mol) and PLGA (average molecular weight of 11,500 g/mol)

(lactide: glycolide = 50:50) were obtained from Sigma-Aldrich (St. Louis, MO, USA). Polyvinyl alcohol (PVA; 98% hydrolyzed, molecular weight ≈ 13,000) was obtained from Acros Organics (Geel, Belgium). Dimethylsulfoxide was purchased from Fisher Chemicals (Fair Lawn, NJ, USA). Tween 80 was purchased from El-Nasr Pharmaceutical Chemicals Co. (Cairo, Egypt). Phosphate-buffered saline (PBS), streptomycin, penicillin, fetal bovine serum, trichloroacetic acid, Dulbecco's modified Eagle's medium, and tris (hydroxymethyl) aminomethane were purchased from Lonza (Basel, Switzerland).

## 2.2 Preparation of Pc-HPCD complex

The Pc-HPCD inclusion complex was synthesized using thin-film hydration techniques, as previously described, with some modifications [8,13]. In brief, Pc was dissolved in methanol in a round-bottom flask. The resulting solution was then subjected to vacuum evaporation using a rotary evaporator, yielding a thin Pc film. Then, the produced thin film was hydrated with 5% (w/v) HPCD solution, followed by 30 min of bath sonication. The molar ratio of Pc:HPCD was 1:1. Subsequently, the mixture solution was placed on a magnetic stirrer for 12 h. The Pc-HPCD complex solution was ultracentrifuged at 15,000 rpm for 15 min (Hermle Z326K, Wehingen, Germany) to eliminate any free drug. The amount of Pc in the Pc-HPCD inclusion complex was quantified using a dual-beam UV-vis spectrophotometer (Peak instruments T-9200, USA) with reference to a calibration curve constructed using a 1:1 (v/v) mixture of Pc dissolved in methanol and 5% HPCD v/v. The complex solution was then subjected to freezedrying using a lyophilizer (TOPTION TOPT-10C Freeze dryer, Toption Group Co., Xi'an, China).

# 2.3 Characterization of the Pc-HPCD inclusion complex

The successful formation of the Pc-HPCD inclusion complex was confirmed before being loaded into PEG/PLGA NPs.

#### 2.3.1 <sup>1</sup>H NMR spectroscopy

<sup>1</sup>H NMR spectroscopy was employed to assess the inclusion complexation between Pc and HPCD. In this regard, free Pc, HPCD powder, and the lyophilized Pc-HPCD complex were studied using a 500 MHz FT-NMR spectrometer (ECA-500, JEOL, Tokyo, Japan) using DMSO as solvent, and chemical shifts ( $\delta$ , ppm) are relative to tetramethylsilane (TMS) using the residual solvent serving as the internal reference when DMSO-d6 is used.

#### 2.3.2 Phase solubility study

The Pc-HPCD inclusion complex was assessed employing the phase solubility study previously described with a few modifications [14,15]. In brief, an excessive amount of Pc was transferred to screw-capped vials containing aqueous solutions with increasing concentrations of HPCD ranging from 0 to 14 mM. Afterward, these mixtures were stirred magnetically for 48 h at 24°C. Subsequently, the resulting mixtures were subjected to centrifugation at 8,000 rpm for 15 min, and the dissolved Pc in the supernatant was quantified after filtration through a 0.45 µm membrane filter at 280 nm using a UV-Vis spectrophotometer (Peak instruments T-9200, USA). The phase solubility diagram (PSD) was constructed by plotting the Pc concentration versus the HPCD concentration. In addition, the stability constant  $(K_s)$  of the Pc-HPCD inclusion complex was estimated using the following equation [16]:

$$K_{\rm S} = \frac{S}{S_0(1-S)},\tag{1}$$

where S is the slope and  $S_0$  is the intrinsic solubility of Pc. In addition, the free energy of the inclusion complex was computed utilizing Gibb's rule, as described in the following equation:

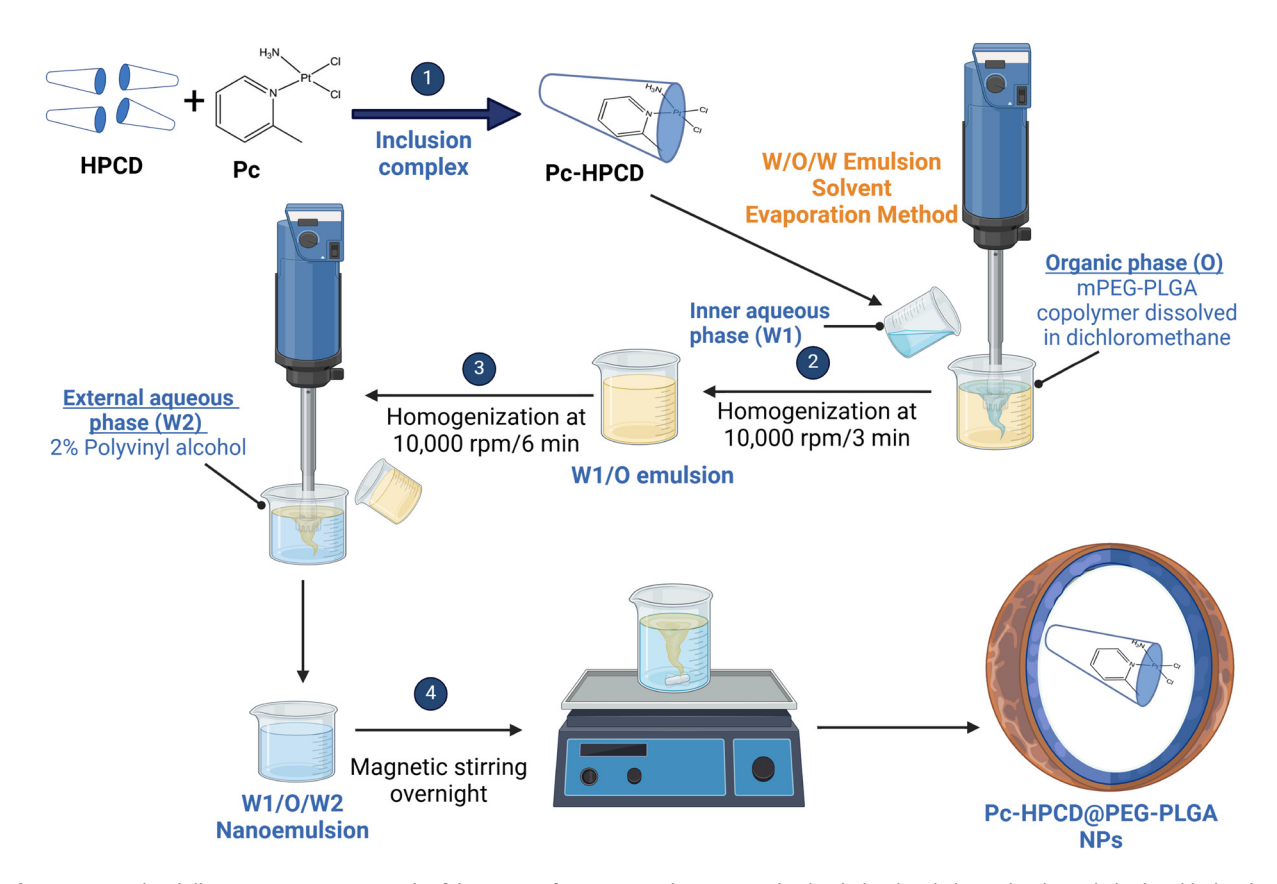
$$\Delta G^{\circ} = -RT \ln k. \tag{2}$$

where  $\Delta G^{\circ}$  is the change in the free energy, R is the universal gas constant, T is the temperature in Kelvin, and k is the stability constant of the complex.

# 2.4 Preparation of Pc-HPCD-loaded core-shell PEG-PLGA nanoparticles (Pc-HPCD@PEG-PLGA NPs)

The loading of the Pc-HPCD inclusion complex into the copolymer mPEG-PLGA NPs was carried out using the modified double water-in-oil-in-water emulsion solvent-evaporation approach (W/O/W), as previously described with modifications (Scheme 2) [8,17,18]. In brief, the organic phase (O) was formed by dissolving 200 mg of the mPEG-PLGA copolymer in 10 mL of the organic solvent (dichloromethane). The inner aqueous phase (W1) was then formed by solubilizing the Pc-HPCD inclusion complex in 100 mL of deionized water. The weight ratio (w/w) of the Pc-HPCD inclusion complex in the W1 phase to mPEG-PLGA

4 — Mohamed S. Nafie et al. DE GRUYTER



**Scheme 2:** Graphical illustration representing the fabrication of Pc-HPCD inclusion complex-loaded poly(ethylene glycol) methyl ether-block-poly (lactide-co-glycolide) core-shell NPs (Pc-HPCD@PEG-PLGA NPs). Created by Biorender.com.

copolymer in the O phase was 0.2:1. Then, the W1 phase was added dropwise to the O phase while homogenizing at 10,000 rpm for 3 min over an ice bath, forming emulsion 1 (W1/O emulsion). Subsequently, emulsion 1 was injected into 50 mL of 2% PVA (external aqueous phase, W2), which acts as an emulsifying agent, homogenizing at 10,000 rpm for 6 min. Finally, the resulting nanoemulsion (W1/O/W2) was magnetically stirred overnight to remove the organic solvent and facilitate NP formation. The obtained core—shell NPs were ultracentrifuged at 11,000 rpm for 30 min at 4°C, washed three times with deionized water and 2.5% w/v sucrose solution, serving as a cryoprotectant, and then lyophilized. The dried NPs were stored at 25°C in a desiccator for further analysis.

#### 2.5 Characterization of NPs

# 2.5.1 Average particle size, PDI, zeta potential, and morphology

At 25°C, the designed Pc-HPCD @PEG-PLGA NPs were assessed for average particle size and PDI using dynamic light scattering, and the surface zeta ( $\zeta$ ) potential was studied employing laser

Doppler velocimetry (Malvern Instruments, Worcestershire, UK) [19–21]. The measurements were based on three independent experiments, and the findings are presented as mean + standard deviation. The morphology of Pc-HPCD@PEG-PLGA NPs was studied using transmission electron microscopy (TEM, JEOL-JEM 2100 electron microscope, Musashino, Akishima, Tokyo, Japan) at an accelerating voltage of 160 kV after staining with 2% phosphotungstic acid [22]. A histogram was then created using the image processing program Image J (NIH, Bethesda, MD, USA), demonstrating the average diameter (nm) of Pc-HPCD@PEG-PLGA NPs.

#### 2.5.2 EE%

EE% was estimated indirectly, as previously described elsewhere, with a few modifications [23–26]. Briefly, the Pc-HPCD@PEG-PLGA NPs were subjected to ultracentrifugation (14,000 rpm, 4°C) for 1 h (Hermle Z 326 K, Labortechnik GmbH, Wehingen, Germany). The unentrapped Pc-HPCD was then quantified in the supernatant at 280 nm using a UV–Vis spectrophotometer (Peak Instruments T-9200, USA). EE% was calculated using equation (3) [27–29]:

$$EE\% = \frac{\text{Total amount of drug - the amount of drug unentrapped}}{\text{Total amount of drug}} \times 100.$$
 (3)

# 2.6 In vitro drug release studies

The dialysis membrane approach was employed to determine the release profile of Pc from Pc-HPCD @PEG-PLGA NPs. Briefly, 1 mL of the Pc-HPCD @PEG-PLGA NPs was placed into a dialysis sac (cut-off molecular weight of 14,000 Da), which was then suspended in a suitable glass bottle containing 25 mL of either PBS or acetate buffer of pH values of 7.4 and 5.5, respectively. The release medium was supplemented with tween (2%) and maintained in a shaking incubator at 150 rpm at 37°C. At specific time intervals, 1 mL of the release medium was pipetted and replaced with an identical volume of fresh pre-warmed PBS or acetate buffer to maintain sink conditions. The amount of Pc was quantified in the pipetted release medium, as described in Section 2.5.

The drug release (%) was determined using equation (4) [30].

Release% = 
$$\frac{\text{Amount of released drug}}{\text{Initial amount of loaded drug}} \times 100\%$$
. (4)

#### 2.7 Cell culture

The invasive triple-negative breast cancer (MDA-MB-231) and the normal breast epithelial cells (MCF-10A) were purchased from ATCC (Wesel, Germany) and maintained as prescribed in our previous work [21].

#### 2.8 Cytotoxicity (SRB assay)

The cytotoxic activities of the free drug Pc, Pc-HPCD complex, and Pc-HPCD@PEG-PLGA NPs were assessed against both cancerous (MDA-MB-231) and normal (MCF10A) breast cells. The cells were incubated with ten different concentrations (0.01, 0.03, 0.1, 0.3, 1, 3, 10, 30, 100, and 300 µg/mL) of the test agents for 48 h, and an SRB assay was performed to evaluate their effects on cellular viability, following a previously described method [23]. The selectivity index (SI) was calculated for each of the investigated agents according to the following equation:

# 2.9 Flow cytometry (apoptosis and cell cycle analysis)

Apoptosis assay and cell cycle analysis were conducted on both untreated MDA-MB-231 cells and those treated with Pc-HPCD@PEG-PLGA NPs at a concentration of 1.6 µg/ml for 48 h. The Annexin V-FITC kit (Abcam Inc., Cambridge, UK) was utilized for the apoptotic estimation, and all procedures were conducted following the manufacturer's guidelines. Cell cycle analysis was performed following a previously described method [21]. ACEA Novocyte™ flow cytometer (ACEA Biosciences Inc., San Diego) was employed for detection in both assays, and its built-in software was used for calculations.

# 2.10 *In vivo* assay

The experiment design, detailed methodology of tumor inoculation, treatments, and blood measurements were carried out following a previously reported procedure, as described in the Supplementary file [31-33]. The experimental protocol summarized in Scheme 3 was approved by the Research Ethics Committee at Suez Canal University (Approval number REC226/2023, Chemistry Department, Faculty of Science, Suez Canal University, Ismailia).

#### 2.11 Statistical analysis

All values were expressed as mean ± SEM or SD. Mean values of different groups were compared using an unpaired Student's t-test using GraphPad Prism software.  $P \le 0.05$  was considered statistically significant.

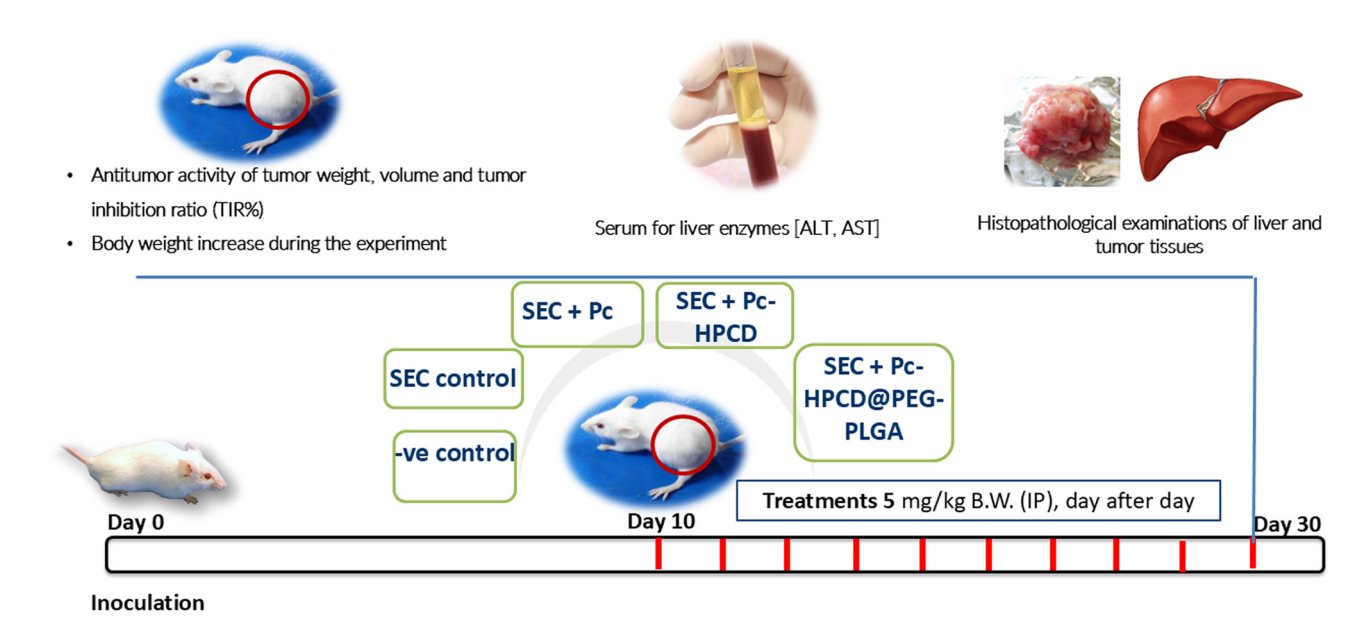
# 3 Results and discussion

# 3.1 Preparation and characterization of the **Pc-HPCD** complex

Our work aims to enhance Pc's water solubility by using a solubilizing host molecule, HPCD. In this context,

$$SI = \frac{\text{Half maximal inhibitory concentration on normal cells (CC50)}}{\text{Half maximal inhibitory concentration on cancer cells (IC50)}}.$$
 (5)

6 — Mohamed S. Nafie et al. DE GRUYTER



Scheme 3: In vivo experiment workflow.

a Pc-HPCD guest-host inclusion complex was prepared, demonstrating improved water solubility. The successful formation of the complex and its enhanced water solubility was confirmed by <sup>1</sup>HNMR and phase solubility study, as detailed in the following sections.

#### 3.1.1 <sup>1</sup>H NMR spectroscopy

Structural elucidation of host-guest complexation supporting the inclusion of Pc within HPCD was carried out via <sup>1</sup>H-NMR spectroscopy at 500 MHz utilizing DMSO as solvent. The changes in proton chemical shifts, explaining the inclusion of Pc within the hydrophobic cavity of HPCD are illustrated in Figure 1 and Table 1. As reported previously, this complex could exhibit one or both of two phases: the ammonia-platinum group pointing toward the inner core of the cavity, thus forming hydrogen bonds with oxygen atoms of pyran rings, or the molecule included with its ammonia-platinum group protruding to the outer portion of the cavity, forming hydrogen bonds with oxygen atoms of outer hydroxyl groups [34]. Both conformers were supported by the literature, and the changes in the chemical shifts are presented in Table 1 [34,35]. Our findings indicated that the protons of ammonia in Pc were shifted from  $\delta$  1.912 to  $\delta$  1.960 Hz with a change of 0.058, which could be due to hydrogen bond formation within the hydrophobic cavity of HPCD. Also, two Pc conformers showed upfield-shifted methyl hydrogens from 4.70 and 4.68 to 3.83 and 3.77 with a change of 0.875 and 0.91, respectively, indicating the effect of inclusion

on Pc conformers. On the other hand, protons of the HPCD were shifted in the range of  $\delta$  5.077–3.416 to  $\delta$  5.060–3.302 Hz with an average change of 0.010. In addition, multiplets of tetrahydropyran hydrogens of O–C from methine have displayed higher shift as an effect of Pc inclusion from 3.52, 3.42 and 3.41 to 3.68, 3.32 and 3.30 with a change of 0.15, 0.10, and 0.12 respectively. The structural elucidation of the host–guest complexation, supported by  $^1$ H-NMR spectroscopy, provided valuable insights into the molecular interactions within the hydrophobic cavity of HPCD. These findings contribute to the understanding of the potential phases and conformers of the complex.

#### 3.1.2 Phase solubility study

A phase solubility study is a beneficial tool for assessing the complexation between host molecules and hydrophobic guest compounds in an aqueous medium. The aqueous solubility of Pc was investigated upon its complexation with HPCD at 25°C, as depicted in Figure 2a and detailed in Table 2. Moreover, the phase solubility study was employed to compute the stoichiometry, stability constant, and free energy of complexation of the Pc-HPCD complex. It was observed that the concentration of Pc increased linearly with an increase in HPCD concentration, suggesting a linear relationship with an  $R^2$  value of 0.97. These data revealed that the solubility of Pc increased by approximately 14-fold compared to its intrinsic solubility upon complexation with HPCD. According to Higuchi and Connors's theory and previous studies, the obtained PSD

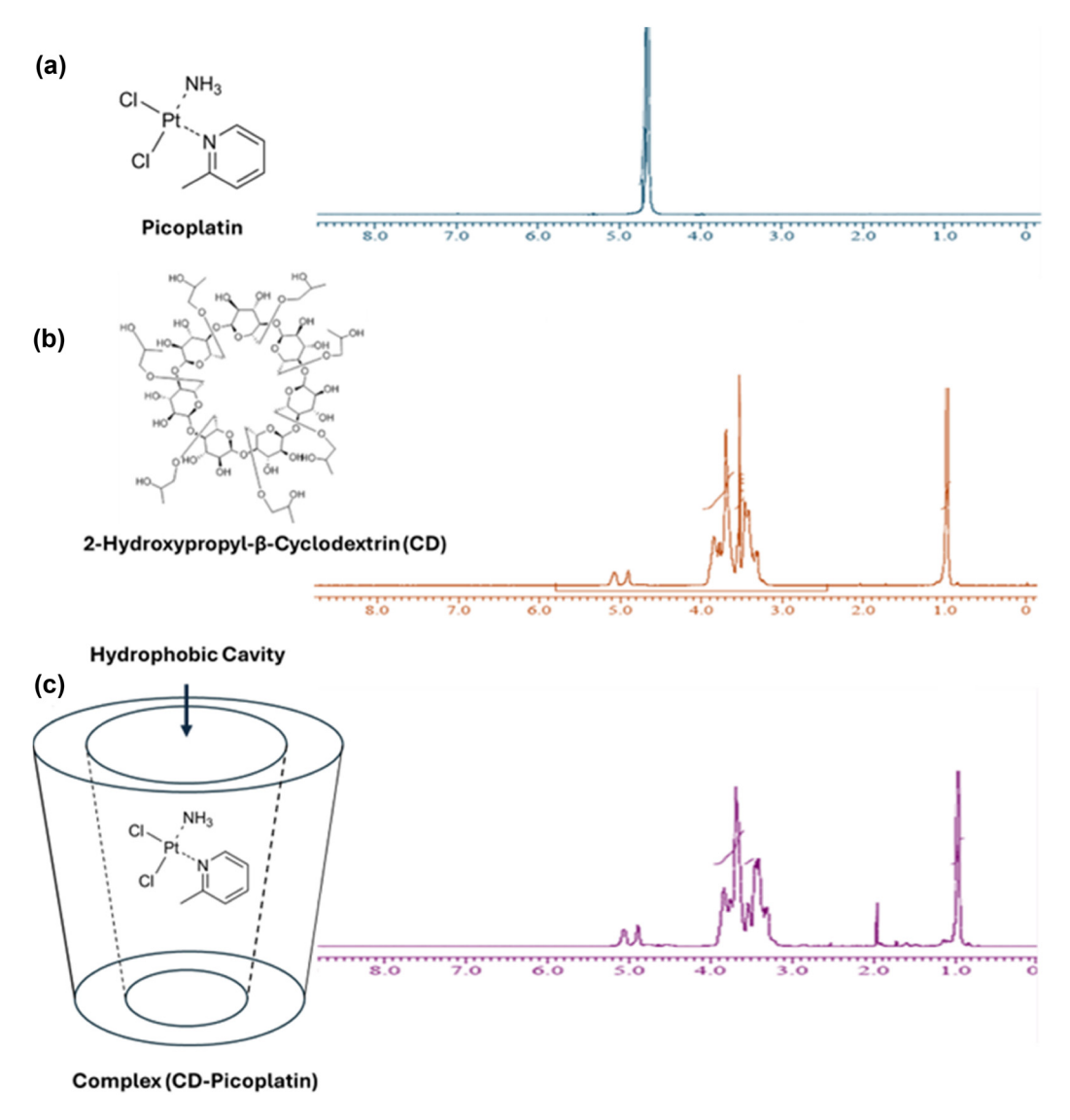


Figure 1: <sup>1</sup>H-NMR spectra of (a) Pc, (b) HPCD, and (c) the Pc-HPCD complex.

follows the AL-type pattern (with 0 < slope < 1), implying a 1:1 stoichiometry between the Pc guest compound and the HPCD host molecule [15,36].

Furthermore, the stability constant (Ks) and complexation-free energy of the Pc-HPCD complex were found to be  $2.7 \times 10^3 \,\mathrm{M}^{-1}$  and  $-4.3 \,\mathrm{kcal} \,\mathrm{mol}^{-1}$ , respectively, as shown in Table 2, indicating the excellent stability of the synthesized complex. The attained values are comparable to previously reported ones (ranging from  $0.04 \times 10^3$  to  $11 \times 10^5$  M<sup>-1</sup>) intended for drug delivery [14,15,36-39]. The phase solubility study provided a comprehensive understanding of the complexation behavior of Pc with HPCD in aqueous medium, elucidating the stoichiometry, stability constant, and free energy of complexation.

# 3.2 Characterization of Pc-HPCD@PEG-**PLGA NPs**

#### 3.2.1 Size, zeta potential, EE, and morphology

The empty and Pc-HPCD-loaded mPEG-PLGA polymeric NPs were engineered using the modified double-emulsion solvent-evaporation approach, wherein the Pc-HPCD inclusion complex was incorporated into the inner aqueous phase. The hydrodynamic diameter, PDI, zeta potential, and EE are presented in Table 3.

The hydrodynamic diameter of the empty PEG-PLGANPs was found to be 161.4  $\pm$  5.3 nm, which increased to 190.2  $\pm$ 8.7 nm after loading with Pc-HPCD. The size increase

**Table 1:** Chemical shifts (ppm) of Pc and HPCD before and after forming the Pc-HPCD complex

		Chemical shift (ppm)			
Protons		δ Ρς	δ 2-hydroxypropyl- β-cyclodextrin	$\delta$ Complex	Δ shift
H-HPCD1	S	_	5.077	5.060	0.010
H-HPCD2	S	_	4.899	4.889	0.010
H-HPCD3	S	_	4.662	4.650	0.012
H-Pc1	S	4.709	_	3.834	0.875
H-Pc2	S	4.680	_	3.770	0.91
H-Pc3	S	4.650	_	4.650	0.0
H-Pc4	S	1.912		1.960	0.058
H-HPCD4	m	_	3.696	3.753	0.057
H-HPCD5	m	_	3.529	3.687	0.158
H-HPCD6	D	_	3.526	3.538	0.012
H-HPCD7	D	_	3.473	3.448	0.025
H-HPCD8	D	_	3.462	3.407	0.043
H-HPCD9	D	_	3.454	3.355	0.099
H-HPCD10	m	_	3.425	3.320	0.105
H-HPCD11	m	_	3.416	3.302	0.124
H-HPCD12	D	_	0.977	0.968	0.009
H-HPCD13	D	_	0.964	0.955	0.009

suggested the successful incorporation of the inclusion complex inside the hydrophilic core of the polymeric NPs [13,18]. Moreover, both empty and loaded polymeric NPs exhibited a monodispersed particle size (0.17  $\pm$  0.03 and 0.14  $\pm$  0.02 nm, respectively).

The zeta potential of the designed empty PEG-PLGANPs showed a high negative surface charge of  $-21.96 \pm 0.80$  mV, indicating the colloidal stability of the prepared NPs. The surface charge changed to  $-13.97 \pm 0.67$  mV after the encapsulation of Pc-HPCD, owing to the cationic nature of Pc [40].

Our findings demonstrated that mPEG-PLGA was successfully emulsified in an aqueous medium to create NPs with a core-shell structure and a size smaller than 200 nm. This size could render them capable of evading recognition and elimination by the reticuloendothelial system, thereby achieving endurance in systemic circulation. In addition, this small size facilitates the enhanced uptake of the NPs by the malignant cells through the enhanced permeability retention effect [41]. The EE% of Pc-HPCD in Pc-HPCD@PEG-PLGA was high (80.7  $\pm$  2.4%). The high EE% could be attributed to the use of a modified double-emulsion solvent-evaporation technique involving a two-step process for the NP preparation. Initially, the W/O nanoemulsion was prepared, entrapping the Pc-HPCD in the aqueous core, followed by producing the W/O/W nanoemulsion in the aqueous phase utilizing the PVA polymer to construct the NPs. This process could limit the leakage of the drug shielded inside the inner aqueous core surrounded by an outer shell [42].

TEM examination revealed the formation of uniform, core–shell spherical polymeric structures with no apparent aggregation (Figure 2b). The observed contrast in the TEM image could be attributed to the staining process carried out using phosphotungstic acid, enabling a clear distinction

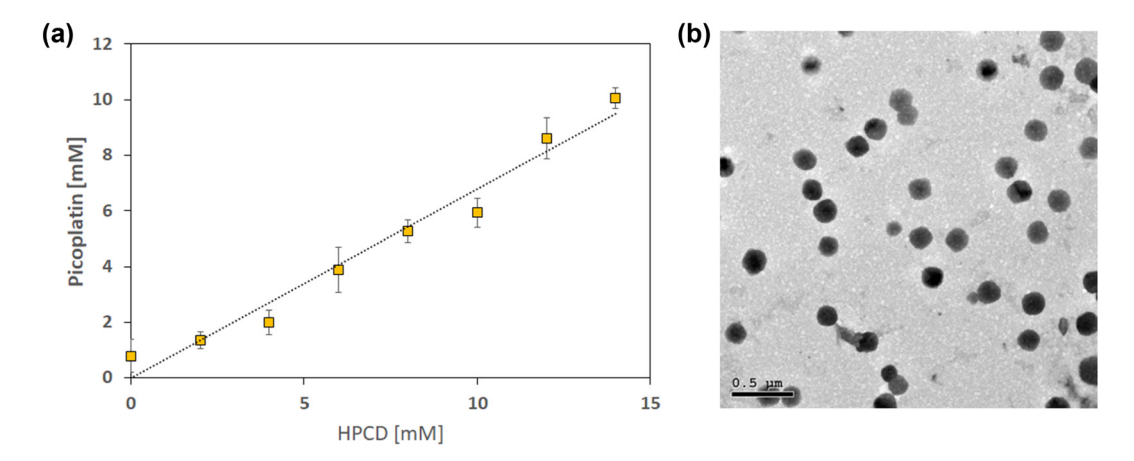


**Figure 2:** (a) PSD of the Pc-HPCD complex at  $\lambda = 280$  nm, and (b) TEM image of Pc-HPCD@PEG-PLGA NPs.

**Table 2:** Stability constant ( $K_s$ ) and complexation-free energy of Pc complexation with HPCD computed from the PSD

	Equation	R <sup>2</sup>	Stability constant $K_s$ (M <sup>-1</sup> )	$\Delta G^{\circ}$ (kcal mol <sup>1</sup> )	PSD type
Pc-HPCD	Y = 0.6802 × - 0.0223	0.97	$2.7 \times 10^3$	-4.3	A <sub>L</sub>

**Table 3:** Characterization of PEG-PLGA NPs; data represent mean  $\pm$  SD (n = 3)

Formula	Diameter (nm)	PDI	Zeta potential (mV)	EE (%)
Empty PEG-PLGA	161.4 ± 5.3	0.17 ± 0.03	-21.96 ± 0.80	_
Pc-HPCD@PEG-PLGA	190.2 ± 8.7	$0.14 \pm 0.02$	−13.97 ± 0.67	$80.7 \pm 2.4$

between the darker outer layer and the lighter inner core. Our findings are consistent with previous studies that utilized the double emulsion method for formulating polymeric NPs [18]. In addition, the average diameter of the NPs was assessed using the Image J software (NIH, Bethesda, MD, USA), and was found to be  $80.2 \pm 13.18 \, \text{nm}$  (Figure 2c). The size of the NPs measured by the dynamic light scattering was larger than that measured by the TEM owing to the Brownian motion of the colloidal NPs. Moreover, the zeta sizer detects the hydraulic size of the NPs, including the water boundary surrounding them [21].

#### 3.2.2 Release study

Controlled drug release is a crucial parameter to consider when formulating various nano-sized delivery systems. Controlled drug release plays a significant role in minimizing undesirable adverse effects by enabling the preferential targeting of drugs to cancerous cells with minimal release in normal cells. The pH-dependent release, an attractive approach for achieving controlled drug release, relies on the selective release of loaded drugs within the acidic cancer microenvironment (pH 4-5.5), following their uptake by the endocytosis mechanism [41,43]. To this end, the in vitro release of Pc-HPCD from Pc-HPCD@PEG-PLGA

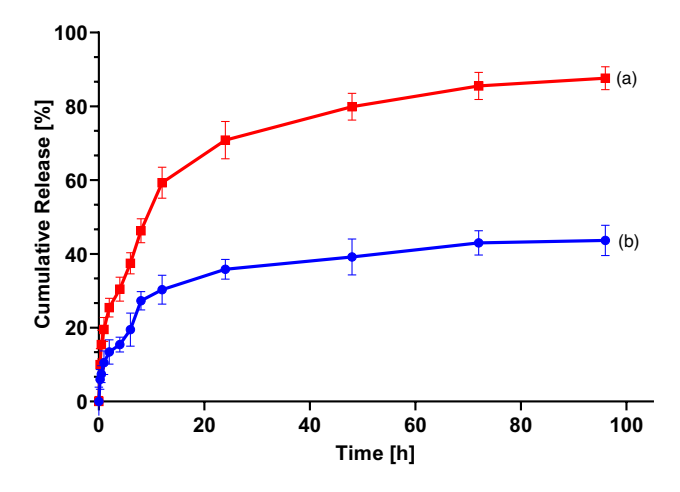


Figure 3: The cumulative release % of Pc-HPCD from Pc-HPCD@PEG-PLGA NPs at (a) pH 5 and (b) pH 7.4. Data represent mean  $\pm$  SD (n = 3).

NPs was studied at two pH values, simulating the acidic tumor microenvironment (pH 5) and physiological conditions (pH 7.4) (Figure 3). The cumulative release of Pc-HPCD at physiological pH was significantly slower than that at acidic pH. Approximately 44 ± 4.1% of Pc-HPCD was released at pH 7.4, as compared to about 87.6 ± 3.2% released at pH 5 within the experimental duration of 96 h. It could be suggested that the release of the loaded drug into the acidic environment was achieved by the erosion of the polymeric matrix, followed by the diffusion of the loaded drug out of the inner aqueous core. In addition, the cleavage of the polymeric ester linkage in the acidic environment may have played a role in rapidly releasing the loaded cargo into the release medium. Our findings showed that our formulation is a promising pH-triggered delivery system capable of selectively releasing its cargo into tumor tissue with minimal release in normal tissue [5,8]. Our findings showed that our formulation is a promising pH-triggered delivery system capable of selectively releasing its cargo into tumor tissue with minimal release in normal tissue.

# 3.3 Cytotoxicity on MDA-MB231 and MCF10A cells

Pc is a new-generation platinum-based anticancer agent with favorable properties that could grant the ability to overcome resistance observed in other platinum drugs [44]. It was previously reported that the complexation of oxaliplatin, a second-generation platinum drug, HPCD, resulted in improved water solubility and enhanced inhibitory effects on the cellular proliferation of breast (MCF-7) and colon (HCT-116) cancer cells [45]. NPs could reduce drug resistance, achieve controlled release, enhance selectivity to cancer cells, and improve the permeability and retention effects [46-49]. The aforementioned benefits that NPs could offer have driven our interest in formulating a Pc-HPCD inclusion complex, incorporating such a complex into PEG-PLGA NPs, and investigating their cytotoxic activity against invasive triple-negative breast cancer (MDA-MB-231) and the normal breast (MCF-10A) cell lines. The newly formulated Pc-HPCD@PEG-PLGA NPs exhibited the lowest half-maximal inhibitory concentration  $(IC_{50} = 1.6 \pm 0.24 \,\mu\text{g/ml})$  against MDA-MB-231 in comparison to

10 — Mohamed S. Nafie et al. DE GRUYTER

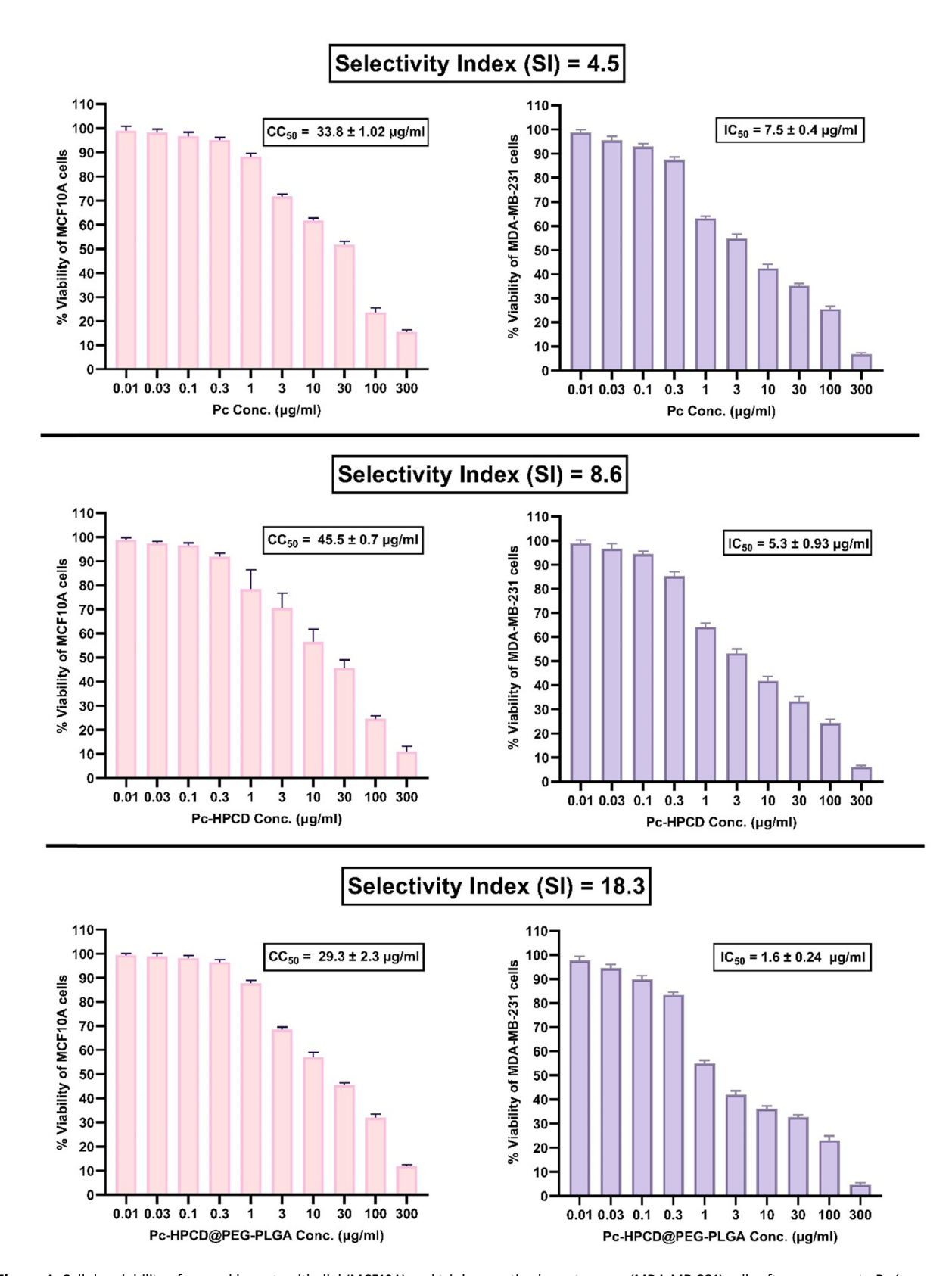


**Figure 4:** Cellular viability of normal breast epithelial (MCF10A) and triple-negative breast cancer (MDA-MB-231) cells after exposure to Pc (top panel), Pc-HPCD (middle panel), and Pc-HPCD@PEG-PLGA NPs (bottom panel) for a duration of 48 h. The displayed data are the average of three experimental runs (n = 3)  $\pm$  standard deviation (SD).

**Table 4:** Apoptosis assay of MDA-MB-231 cells following 48 h of exposure to Pc-HPCD@PEG-PLGA treatment

Apoptotic stage of MDA-MB-231	Control (untreated)	Pc-HPCD@PEG-PLGA NPs (1.6 µg/mL)
Necrosis (Q2-1) (AV-/PI+)	1.8 ± 0.11	***20.62 ± 3.10
Late apoptosis (Q2-2) (AV+/PI +)	1.05 ± 0.05	***14.13 ± 0.46
Viable cells (Q2-3) (AV-/PI-)	97.01 ± 0.09	***63.09 ± 2.65
Early apoptosis (Q2-4) (AV+/PI-)	0.14 ± 0.03	***2.17 ± 0.40

treatment with Pc-HPCD or free Pc (Figure 4). The detected IC50s for free Pc and Pc-HPCD on MDA-MB-231 cancerous cells

were  $7.5 \pm 0.4$  and  $5.3 \pm 0.93 \,\mu\text{g/ml}$ , respectively (Figure 4). The results obtained indicated that the complexation of Pc with HPCD increased the cytotoxic activity of Pc against cancer cells by 1.4-fold, whereas the loading of Pc-HPCD onto PEG-PLGA NPs potentiated the cytotoxic activity of Pc against cancer cells by 4.7-fold. These findings highlighted the synergistic effects of both complexation and NP delivery systems in enhancing the therapeutic efficacy of Pc against cancer cells. Cytotoxicity of the three investigated agents (Pc, Pc-HPCD, and Pc-HPCD@PEG-PLGA NPs) was also tested against normal breast epithelial cell lines (MCF-10A), and their half-maximal inhibitory concentrations (CC<sub>50</sub>) were determined, as shown in Figure 4, to assess the SI. The SI serves as an indicative measure of the drug's ability to harm cancer cells while preserving the normal counterparts. High SI values are typically associated with higher selectivity toward cancer cells [5]. The SI of Pc toward MDA-MB-231 cancer cells was 4.5, which nearly doubled with Pc-

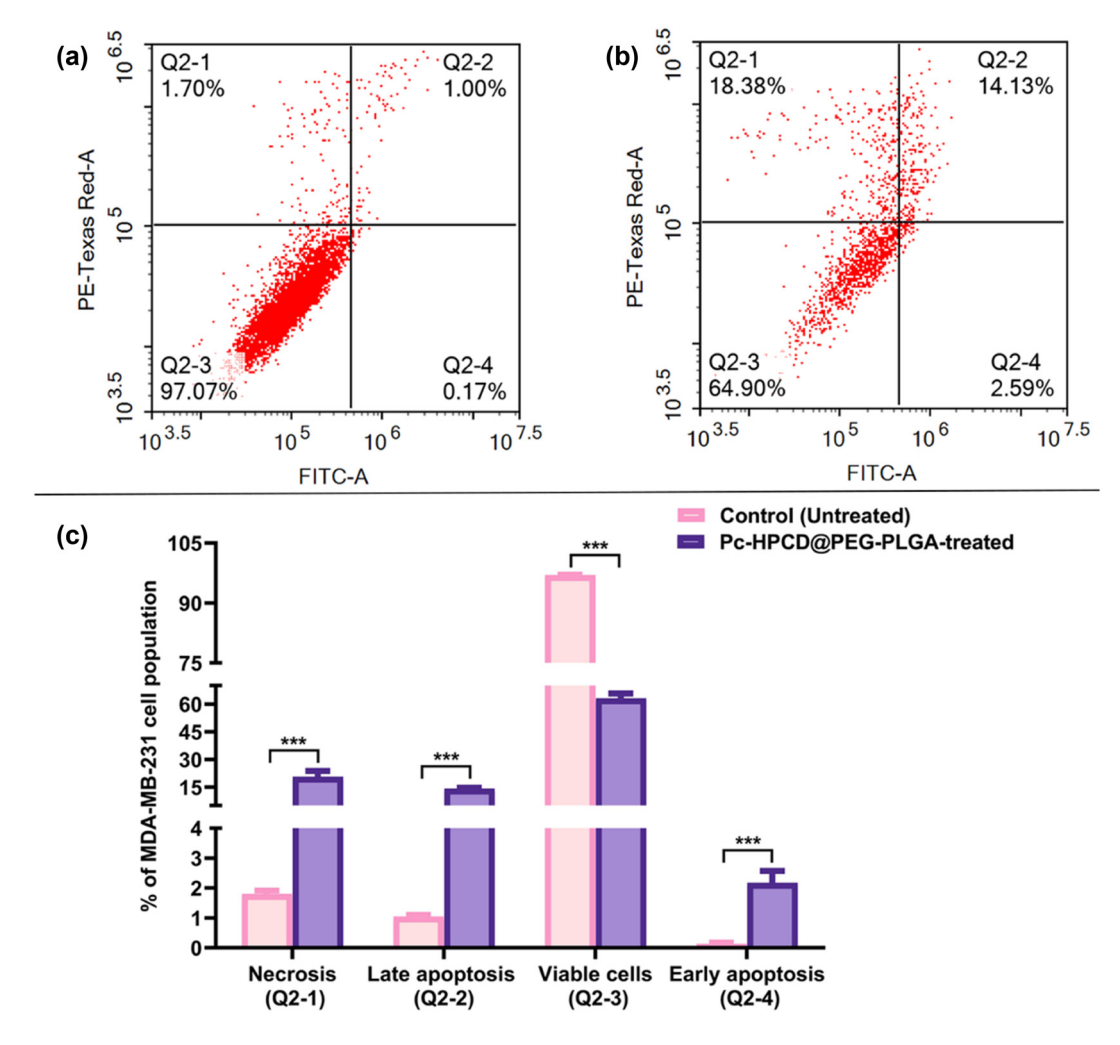


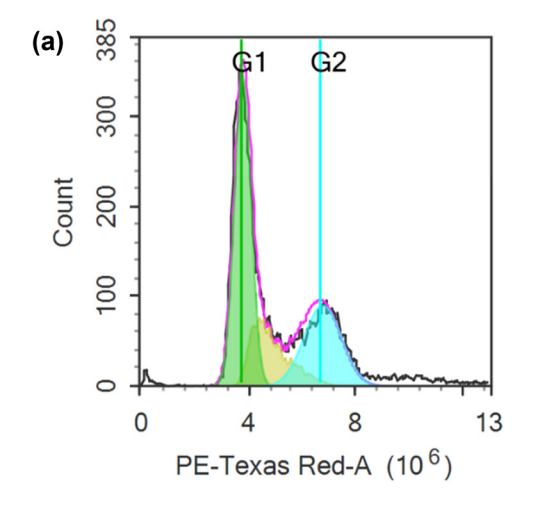
**Figure 5:** Apoptosis in MDA-MB-231 cells. (a) Cytogram displaying untreated MDA-MB-231 cells, (b) cytogram showing MDA-MB-231 cells after incubation with Pc-HPCD@PEG-PLGA NPs for 48 h, (c) bar graph presenting the quadrant analysis for both untreated and Pc-HPCD@PEG-PLGA treated MDA-MB-231 cells. Data are presented as the average triplicates ± standard deviation (SD). \*\*\* p-value ≤0.0005 from the control (untreated).

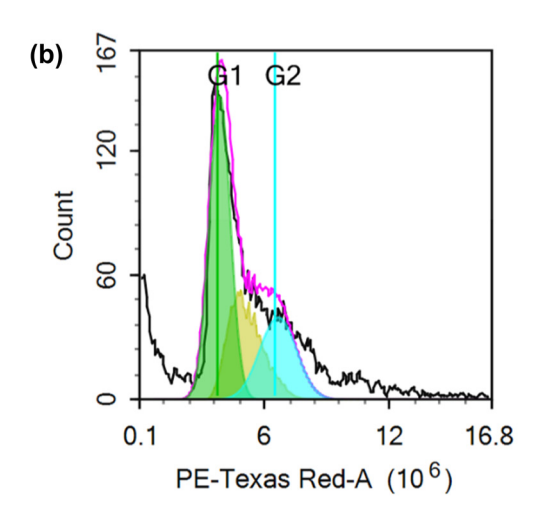
**Table 5:** Cell cycle analysis of MDA-MB-231 cells following 48 h of exposure to Pc-HPCD@PEG-PLGA as compared to control (untreated cells)

Cell cycle phase of MDA-MB-231	Control (Untreated)	Pc-HPCD@PEG-PLGA NPs (1.6 µg/mL)
Sub-G1	1.26 ± 0.22	***10.80 ± 0.22
G1	46.84 ± 1.06	*41.88 ± 1.54
S	19.72 ± 0.14	21.74 ± 0.26
G2	27.74 ± 0.83	***19.42 ± 0.94

HPCD, reaching an SI of 8.6. However, Pc-HPCD@PEG-PLGA NPs showed the highest SI (18.3) against MDA-MB-231 cancer cells (Figure 4), reflecting the highest safety margin among all investigated agents. This observation indicated a significantly

improved safety margin compared to Pc-HPCD or uncomplexed Pc, highlighting the potential of NP formulations in minimizing adverse effects on normal cells while effectively targeting cancerous cells. The improved cytotoxic effects of the engineered NPs against TNBCs while maintaining minimum toxic effects against normal cells are attributed to their nanoscale dimensions (<200 nm), which facilitate the passive transport of the NPs through the leaky vasculature of neoplastic cells. This leads to the preferential uptake of the NPs into tumor cells, resulting in higher internalization of Pc into cancerous cells, as compared to healthy ones [50]. The formulation of Pc-HPCD@PEG-PLGA NPs not only significantly potentiated the cytotoxic activity of Pc against cancer cells but also exhibited the highest SI, suggesting a promising strategy for improving the therapeutic efficacy and safety profile of platinum-based anticancer agents.





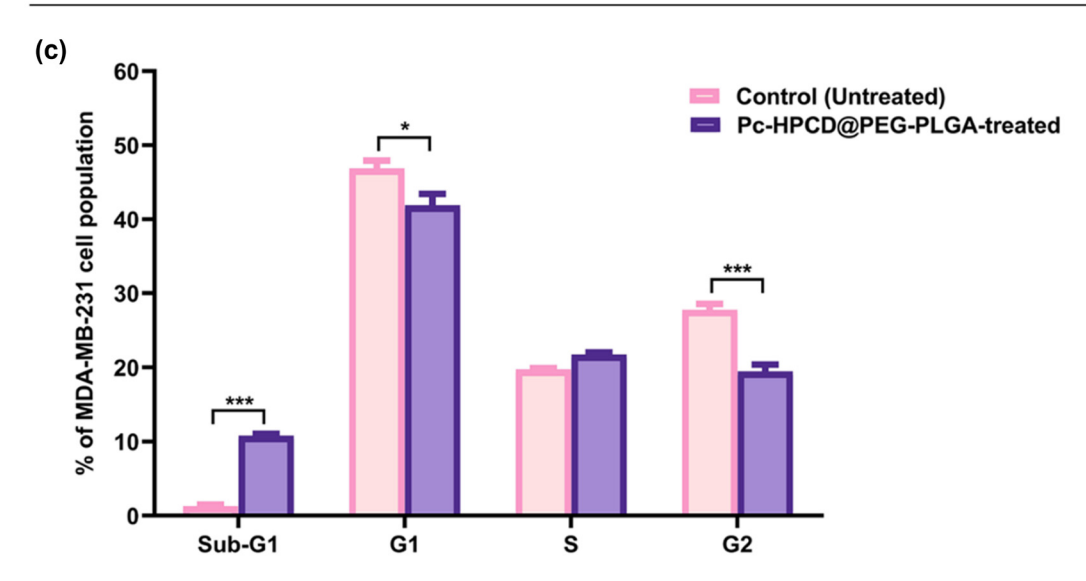


**Figure 6:** Cytograms showing the cell cycle kinetics of MDA-MB-231 untreated (control) cells (a), MDA-MB-231 cells treated with Pc-HPCD@PEG-PLGA NPs for 48 h (b), and a bar graph showing the frequency of cells at each of the different phases of the cell cycle (c). Data are presented as the average of triplicates  $\pm$  standard deviation (SD). \* and \*\*\* represent p-values  $\le$ 0.05 and  $\le$ 0.0005, respectively.

Table 6: Antitumor parameters in untreated and treated SEC-bearing mice

	SEC control	SEC + Pc	SEC + Pc-HPCD	SEC + Pc-HPCD@PEG-PLGA
Tumor inhibition ratio (TIR%)	_	18.77 <sup>#</sup> ± 1.0	32.19 <sup>#</sup> ± 1.01	67.17 <sup>#</sup> ± 1.1

Picoplatin (Pc), Picoplatin/β-hydroxy propyl cyclodextrin (Pc-HPCD), and Picoplatin/β-hydroxy propyl cyclodextrin loaded PEG-PLGA (Pc-HPCD@PEG-PLGA NPs). Values are expressed as "Mean  $\pm$  SD" values of mice in each group (n = 5). # values are significantly different ( $P \le 0.05$ ) between treated SEC and SEC control mice using the unpaired test in GraphPad prism". TIR% =  $C - T/C \times 100$ .

# 3.4 Flow cytometry (apoptosis and cell cycle analysis)

The cell viability studies demonstrated significant cytotoxic activity of Pc-HPCD@PEG-PLGA against MDA-MB-231 cells. To better understand the intracellular pathways through which the formulated complex induced cell death, flow cytometric apoptotic analysis was conducted on the MDA-MB-231 cells following treatment with Pc-HPCD@PEG-PLGA. Pc-HPCD@PEG-PLGA NPs showed high potential in activating both apoptotic and necrotic pathways. Pc-HPCD@PEG-PLGA increased the percentage of the cellular population in both early and late apoptosis quadrants by 15.5- and 13.5-fold, respectively, compared to the control (untreated) cells. Additionally, Pc-HPCD@PEG-PLGA NPs increased the frequency of necrotic MDA-MB-231 cells by 11.5-fold relative to the control (Table 4, Figure 5). Moreover, the viable cells quadrant witnessed approximately a 35% reduction upon treatment with Pc-HPCD@PEG-PLGA NPs for 48 h (Table 4, Figure 5). These findings highlighted the remarkable ability of our innovative formulation to induce both apoptosis and necrosis while significantly reducing the viability of the aggressive TNBC (MDA-MB-231), as illustrated in Figure 5.

Cell cycle analyses were performed to detect the frequency of MDA-MB-231 cells at each phase of the cell cycle after 48 h incubation with Pc-HPCD@PEG-PLGA NPs as compared to the control (untreated MDA-MB-231 cells). Pc-HPCD@PEG-PLGA NPs resulted in significant sequestration of cells at the sub-G1 phase (p-value  $\leq 0.0005$ ) and a notable reduction in the frequency of cells at both G1 (p-value  $\leq 0.05$ ) and G2 phases (p-value  $\leq 0.0005$ ) compared to the control (Table 5 and Figure 6). The presence of low molecular weight DNA, represented by the sub-G1 phase, is typically associated with apoptosis. Accordingly, the ability of Pc-HPCD@PEG-PLGA NPs to trap cellular population at the sub-G1 phase highlighted its pronounced apoptotic effects.

The cell viability studies and flow cytometric apoptotic analysis illustrated the significant cytotoxic activity of Pc-HPCD@PEG-PLGA against MDA-MB-231 cells. The high efficacy of Pc-HPCD@PEG-PLGA to activate both apoptotic and necrotic pathways was evident, with a remarkable increase in the percentage of cellular population in both early and late

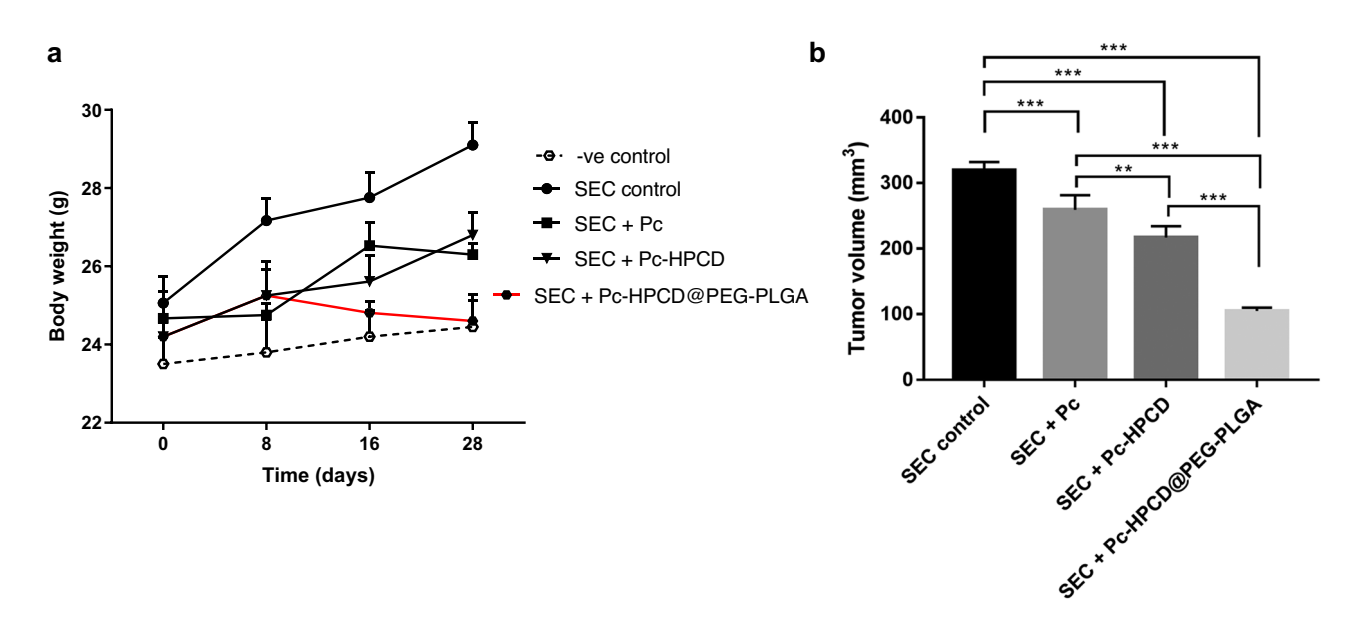


Figure 7: Assessment of anti-tumor potentiality of Pc, Pc-HPCD, and Pc-HPCD@PEG-PLGA against SEC-bearing mice. The increase in mice weight during the experiment (a); Tumor volume (b). Values are expressed as Mean  $\pm$  SD (n = 5). \*p < 0.05, \*\*p < 0.01, \*\*\*p < 0.001.

apoptosis quadrants and a substantial increase in the frequency of necrotic cells. These findings collectively demonstrate the high ability of the newly formulated complex to induce both apoptosis and necrosis, leading to a significant reduction in the viability of aggressive TNBC (MDA-MB-231).

## 3.5 In vivo study

The *in vivo* anticancer activity of Pc, Pc-HPCD, and Pc-HPCD@PEG-PLGA NPs was assessed in solid Ehrlich tumor-bearing female Swiss albino mice. The untreated tumor-bearing mice were employed as a control. On day 10 post tumor cell inoculation, the other mice groups were intraperitoneally injected Pc, Pc-HPCD, or Pc-HPCD@PEG-PLGA at 5 mg PC/kg bodyweight on a daily basis. The treatment with Pc, Pc-HPCD, Pc-HPCD@PEG-PLGA NPs demonstrated a significant antitumor effect, leading to reductions in solid tumor mass (Figure 7).

The measured tumor volume decreased from  $319.32 \pm 12.92 \text{ mm}^3$  in untreated mice to  $259.20 \pm 22.46$ ,  $216.84 \pm 17.34$ , and  $104.82 \pm 5.15 \text{ mm}^3$  with Pc, Pc-HPCD, and Pc-HPCD@PEG-PLGA treatments, respectively. The results showed that treatments with Pc, Pc-HPCD, and Pc-HPCD@PEG-PLGA NPs inhibited tumor proliferation by  $18.77 \pm 1.0\%$ ,  $32.19 \pm 1.01\%$ , and  $67.17 \pm 1.1\%$ , respectively (Table 6).

To assess the impact of the treatments administered during the tumor therapy experiment on the animals'

blood composition, the counts of RBCs, WBCs, and hemoglobin levels in the blood collected from mice were determined (Figure 8). Compared with the healthy mice, untreated tumor-bearing mice demonstrated a significantly lower RBC count and hemoglobin level. Conversely, the RBC count and hemoglobin levels detected in blood samples collected from Pc-HPCD@PEG-PLGA NPs-treated tumor-bearing mice were significantly higher than those detected in untreated tumor-bearing mice, approaching normal values. These observations suggested the potential therapeutic benefit of Pc-HPCD@PEG-PLGA NP treatment in restoring hematological parameters toward normal levels. Furthermore, the WBC count in Pc-HPCD@PEG-PLGA NP-treated mice was comparable to that in healthy mice. These effects are attributed to the ability of the NPs to suppress tumor cell proliferation and serve as a chemoprotective agent.

AST and ALT are predominantly present in the liver, and heightened levels can indicate liver damage. Monitoring the liver enzymes aids in detecting potential hepatotoxicity caused by cancer treatments. Furthermore, increased levels of liver enzymes may serve as an indicator of liver metastasis or other underlying health concerns. As shown in Figure 3b, the ALT and AST levels in blood samples collected from untreated tumor-bearing mice were significantly increased to 80.6 and 79.6 U/L, respectively, due to hepatocellular damage induced following tumor inoculation. However, significantly lower ALT and AST levels were detected in mice treated with Pc-HPCD@PEG-PLGA compared to the untreated tumor-bearing mice. This decrease in liver enzyme levels following treatment

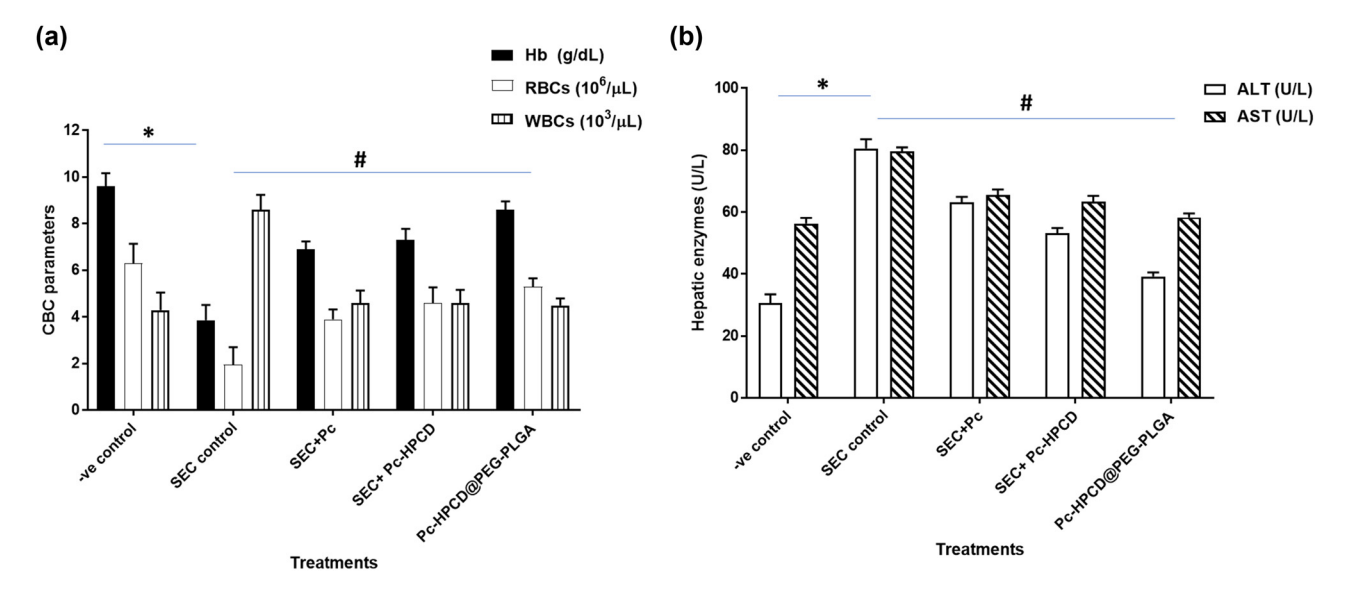


**Figure 8:** Hematological (CBC parameters) (a) and biochemical assessment alanine transaminase and aspartate aminotransferase (ALT and AST) parameters (b) in untreated and treated SEC-bearing mice. Values are expressed as mean  $\pm$  SD of five independent trials. \* $P \le 0.05$  was significantly different between normal and SEC control groups, while  $^{\#}P \le 0.05$  was significantly different between SEC control and SEC-treated groups.

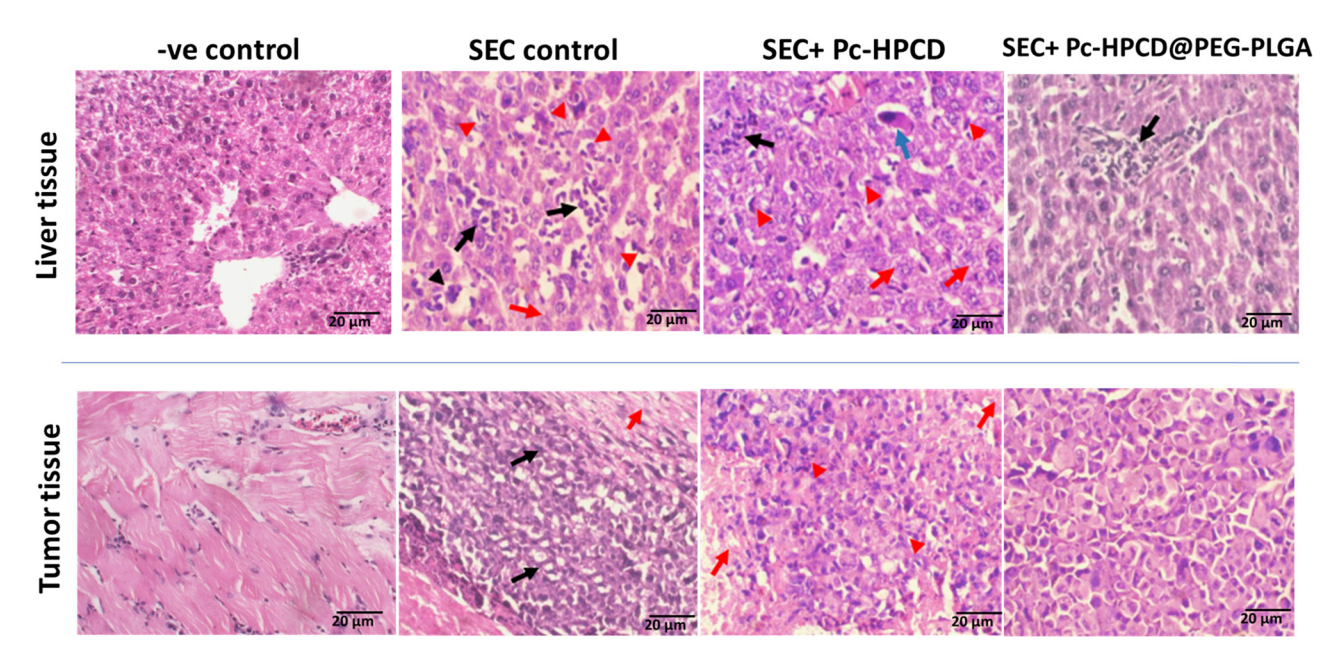


Figure 9: Histopathological examinations of liver tissues and tumor tissues of untreated and treated SEC-bearing mice (H and E stain, magnification ×40), Lobular inflammation (black arrows), area of necrosis (black arrowhead), hydropic degeneration (red arrows), apoptotic cells (red arrowheads), and cell transformation (blue arrow).

suggests a protective effect of Pc-HPCD@PEG-PLGA on the liver. It could imply that the treatment had a positive impact on mitigating liver damage associated with the tumor or potentially reducing the toxic effects of the tumor on the liver as compared to SEC control. These results demonstrated improvements in hematological and biochemical measurements and highlighted the antitumor potentiality of HPCD@PEG-PLGA.

Furthermore, histopathological examinations of liver tissues dissected from untreated SEC-bearing mice revealed foci of lobular inflammation (black arrows) (Figure 9). There was an area of necrosis (black arrowhead) with the replacement of hepatocytes by chronic inflammatory cells. Many hepatocytes show hydropic degeneration (red arrows), and scattered apoptotic cells (red arrowheads) were observed. Conversely, upon treatment with Pc-HPCD@PEG-PLGA NPs, liver tissue showed fewer foci of lobular inflammation (black arrows) with no areas of necrosis. There was no evidence of hydropic degeneration or apoptotic hepatocytes in Pc-HPCD@PEG-PLGA NP-treated mice. These results suggest a protective effect of the treatment on liver tissue integrity and function, possibly by mitigating the inflammatory response induced by the tumor. Moreover, histopathological examination of tumor tissue dissected from untreated SEC-bearing mice exhibited sheets of malignant epithelial cells (black arrows), showing cellular and nuclear pleomorphism, nuclear hyperchromasia, and an increased nucleo-cytoplasmic ratio. Tumor cells infiltrated skeletal muscle bundles, and upon treatment with PcHPCD@PEG-PLGA, there was a decrease in cellular and nuclear pleomorphism, suggesting a potential therapeutic effect in reducing cellular abnormalities and slowing down tumor growth. The histopathological findings supported the potential efficacy of Pc-HPCD@PEG-PLGA NPs in mitigating liver damage and slowing down tumor progression in SECbearing mice.

# 4 Conclusions

The double-emulsion solvent evaporation approach was utilized to formulate PEG-PLGA core-shell NPs encapsulating the Pc-HPCD inclusion complex. The complex was well settled in the inner aqueous core, exhibiting a pHtriggered release behavior. This approach holds promise in tumor therapy as the loaded anticancer complex showed higher release in an acidic medium rather than neutral pH, mimicking the tumor microenvironment simulating the normal physiological conditions. In addition, Pc-HPCD@PEG-PLGA exhibited the highest cytotoxic activity and SI against MDA-MB-231 cancer cells compared to free Pc or the Pc-HPCD complex alone. Pc-HPCD@PEG-PLGA NPs also demonstrated considerable apoptotic and necrotic activities, as evidenced by their significant ability to trap cells at the sub-G1 phase and prevent the cell cycle progression in breast cancer cells. In vivo experiments showed that the treatment with PcHPCD@PEG-PLGA NPs resulted in a 67.2% reduction in tumor growth while improving hematological and biochemical parameters as well as maintaining the normal histopathological architecture. In conclusion, this study provides the feasibility of a novel anticancer core—shell polymeric system in a pH-triggered release manner that can execute TNBC *via* inducing apoptosis while maintaining minimum toxic effects on normal cells. Thus, our NPs are promising in advancing more progressive strategies in cancer therapy.

**Acknowledgments:** The authors acknowledge the efforts of Dr. Wael A. Hassan, A. Professor of Pathology at the College of Medicine, Suez Canal University, and Manager of Alawael Private Pathology Laboratory for Histopathology Diagnosis, for conducting the histopathological examinations and providing their interpretation.

**Funding information:** Dr. Sherif Ashraf Fahmy acknowledges the financial support and sponsorship received from the Alexander von Humboldt Foundation, Germany. Also, Open Access funding was provided by the Open Access Publishing Fund of Philipps-Universität Marburg to Prof. Udo Bakowsky.

**Author contributions:** Conceptualization, Udo Bakowsky and Sherif Ashraf Fahmy; data curation, Mohamed S. Nafie, Nada K. Sedky, Hatem A.F.M. Hassan, Iten M. Fawzy, Manal M. M. Abdelhady, Udo Bakowsky, and Sherif Ashraf Fahmy; formal analysis, Mohamed S. Nafie, Nada K. Sedky, Hatem A.F.M. Hassan, Iten M. Fawzy, Manal M. M. Abdelhady, Udo Bakowsky, and Sherif Ashraf Fahmy; funding acquisition, Udo Bakowsky and Sherif Ashraf Fahmy; investigation, Mohamed S. Nafie, Nada K. Sedky, Hatem A.F.M. Hassan, Iten M. Fawzy, Udo Bakowsky, and Sherif Ashraf Fahmy; methodology, Mohamed S. Nafie, Nada K. Sedky, Hatem A.F.M. Hassan, Iten M. Fawzy, and Sherif Ashraf Fahmy; project administration, Udo Bakowsky and Sherif Ashraf Fahmy; resources, S.A.F. and U.B.; software, Mohamed S. Nafie, Nada K. Sedky, Hatem A.F.M. Hassan, Iten M. Fawzy, Manal M. M. Abdelhady, and Sherif Ashraf Fahmy; supervision, Udo Bakowsky and Sherif Ashraf Fahmy; validation, Udo Bakowsky and Sherif Ashraf Fahmy.; writing - original draft, Mohamed S. Nafie, Nada K. Sedky, Hatem A.F.M. Hassan, Iten M. Fawzy, Udo Bakowsky, and Sherif Ashraf Fahmy; writing - review and editing, S Mohamed S. Nafie, Nada K. Sedky, Hatem A.F.M. Hassan, Iten M. Fawzy, Manal M. M. Abdelhady, Udo Bakowsky, and Sherif Ashraf Fahmy. All authors have accepted responsibility for the entire content of this manuscript and approved its submission.

**Conflict of interest:** The authors state no conflict of interest.

**Ethical approval:** The research related to animal use has been complied with all the relevant national regulations and institutional policies for the care and use of animals.

**Data availability statement:** All data generated or analyzed during this study are included in this published article.

#### References

- [1] Fahmy SA, Dawoud A, Zeinelabdeen YA, Kiriacos CJ, Daniel KA, Eltahtawy O, et al. Molecular engines, therapeutic targets, and challenges in pediatric brain tumors: a special emphasis on hydrogen sulfide and rna-based nano-delivery. Cancers. 2022;14:5244.
- [2] Ayoub AM, Atya MS, Abdelsalam AM, Schulze J, Amin MU, Engelhardt K, et al. Photoactive Parietin-loaded nanocarriers as an efficient therapeutic platform against triple-negative breast cancer. Int J Pharm. 2023;643:123217.
- [3] Fahmy SA, Ponte F, Grande G, Fawzy IM, Mandour AA, Sicilia E, et al. Synthesis, characterization and host-guest complexation of asplatin: improved in vitro cytotoxicity and biocompatibility as compared to cisplatin. Pharmaceuticals. 2022;15:259.
- [4] Ritacco I, Al Assy M, Abd El-Rahman MK, Fahmy SA, Russo N, Shoeib T, et al. Hydrolysis in acidic environment and degradation of satraplatin: a joint experimental and theoretical investigation. Inorg Chem. 2017;56:6013–26.
- [5] Sedky NK, Arafa KK, Abdelhady MMM, Issa MY, Abdel-Kader NM, Mahdy NK, et al. Nedaplatin/peganum harmala alkaloids co-loaded electrospun, implantable nanofibers: a chemopreventive nanodelivery system for treating and preventing breast cancer recurrence after tumorectomy. Pharmaceutics. 2023;15:2367.
- [6] Fahmy SA, Preis E, Dayyih AA, Alawak M, El-Said Azzazy HM, Bakowsky U, et al. Thermosensitive liposomes encapsulating nedaplatin and picoplatin demonstrate enhanced cytotoxicity against breast cancer cells. ACS Omega. 2022;7:42115–25.
- [7] Holford J, Raynaud F, Murrer BA, Grimaldi K, Hartley JA, Abrams M, et al. Chemical, biochemical and pharmacological activity of the novel sterically hindered platinum co-ordination complex, cis-[amminedichloro(2-methylpyridine)] platinum(II) (AMD473). Anticancer Drug Des. 1998;13:1–18.
- [8] Fahmy SA, Mahdy NK, Al Mulla H, ElMeshad AN, Issa MY, Azzazy HME. PLGA/PEG nanoparticles loaded with cyclodextrinpeganum harmala alkaloid complex and ascorbic acid with promising antimicrobial activities. Pharmaceutics. 2022;14:142.
- [9] Liang B, Hao J, Zhu N, Han L, Song L, Hong H. Formulation of nitrendipine/hydroxypropyl-β-cyclodextrin inclusion complex as a drug delivery system to enhance the solubility and bioavailability by supercritical fluid technology. Eur Polym J. 2023;187:111880.
- [10] Mai Y, Eisenberg A. Self-assembly of block copolymers. Chem Soc Rev. 2012;41:5969–85.
- [11] Rafiei P, Haddadi A. Docetaxel-loaded PLGA and PLGA-PEG nanoparticles for intravenous application: pharmacokinetics and biodistribution profile. Int J Nanomed. 2017;12:935–47.
- [12] Mares AG, Pacassoni G, Marti JS, Pujals S, Albertazzi L. Formulation of tunable size PLGA-PEG nanoparticles for drug delivery using microfluidic technology. PLoS One. 2021;16:e0251821.

- [13] Plenagl N, Seitz BS, Duse L, Pinnapireddy SR, Jedelska J, Brussler J, et al. Hypericin inclusion complexes encapsulated in liposomes for antimicrobial photodynamic therapy. Int J Pharm. 2019;570:118666.
- [14] Ponte F, Sedky NK, Fawzy IM, Mokhtar F, Sicilia E, Fahmy SA. Psoralidin-cucurbit[7]uril complex with improved solubility to tackle human colorectal cancer: experimental and computational study. Mater Adv. 2023;4:5324-37.
- [15] Mader WJ, Higuchi T. Phase solubility analysis. Crit Rev Anal Chem. 1970;1:193-215.
- [16] Fahmy SA, Nematallah KA, Mahdy NK, El-Askary HI, Meselhy MR, El-Said Azzazy HM. Enhanced antioxidant, antiviral, and anticancer activities of the extract of fermented egyptian rice bran complexed with hydroxypropyl-beta-cyclodextrin. ACS Omega. 2022:7:19545-54.
- [17] Haggag Y, Abdel-Wahab Y, Ojo O, Osman M, El-Gizawy S, El-Tanani M, et al. Preparation and in vivo evaluation of insulinloaded biodegradable nanoparticles prepared from diblock copolymers of PLGA and PEG. Int | Pharm. 2016;499:236-46.
- [18] Wang H, Zhao Y, Wu Y, Hu YL, Nan K, Nie G, et al. Enhanced antitumor efficacy by co-delivery of doxorubicin and paclitaxel with amphiphilic methoxy PEG-PLGA copolymer nanoparticles. Biomaterials. 2011;32:8281-90.
- [19] Fahmy SA, Ramzy A, Sawy AM, Nabil M, Gad MZ, El-Shazly M, et al. Ozonated olive oil: enhanced cutaneous delivery via niosomal nanovesicles for melanoma treatment. Antioxidants (Basel). 2022;11(7):1318.
- [20] Youness RA, Al-Mahallawi AM, Mahmoud FH, Atta H, Braoudaki M, Fahmy SA. Oral delivery of psoralidin by mucoadhesive surfacemodified bilosomes showed boosted apoptotic and necrotic effects against breast and lung cancer cells. Polymers. 2023;15:1464.
- [21] Fahmy SA, Sedky NK, Ramzy A, Abdelhady MMM, Alabrahim OAA, Shamma SN, et al. Green extraction of essential oils from Pistacia lentiscus resins: Encapsulation into Niosomes showed improved preferential cytotoxic and apoptotic effects against breast and ovarian cancer cells. J Drug Delivery Sci Technol. 2023;87:104820.
- [22] Fahmy SA, Fawzy IM, Saleh BM, Issa MY, Bakowsky U, Azzazy HME. Green synthesis of platinum and palladium nanoparticles using peganum harmala I. seed alkaloids: biological and computational studies. Nanomaterials (Basel). 2021;11(4):965.
- [23] Sedky NK, Abdel-Kader NM, Issa MY, Abdelhady MMM, Shamma SN, Bakowsky U, et al. Co-delivery of ylang ylang oil of cananga odorata and oxaliplatin using intelligent ph-sensitive lipidbased nanovesicles for the effective treatment of triple-negative breast cancer. Int J Mol Sci. 2023;24(9):8392.
- [24] Azzazy HME-S, Sawy AM, Abdelnaser A, Meselhy MR, Shoeib T, Fahmy SA. Peganum harmala alkaloids and tannic acid encapsulated in PAMAM dendrimers: improved anticancer activities as compared to doxorubicin. ACS Appl Polym Mater. 2022;4:7228-39.
- [25] Attia RT, Ewida MA, Khaled E, Fahmy SA, Fawzy IM. Newly synthesized anticancer purine derivatives inhibiting p-eif4e using surfacemodified lipid nanovesicles. ACS Omega. 2023;8:37864-81.
- [26] AbuBakr AH, Hassan H, Abdalla A, Khowessah OM, Abdelbary GA. Therapeutic potential of cationic bilosomes in the treatment of carrageenan-induced rat arthritis via fluticasone propionate gel. Int J Pharm. 2023;635:122776.
- [27] Yuan JH, Yang F, Wang F, Ma JZ, Guo YJ, Tao QF, et al. A long noncoding RNA activated by TGF-beta promotes the invasionmetastasis cascade in hepatocellular carcinoma. Cancer Cell. 2014:25:666-81.

- [28] Tzeyung AS, Md S, Bhattamisra SK, Madheswaran T, Alhakamy NA, Aldawsari HM, et al. Fabrication, optimization, and evaluation of rotigotine-loaded chitosan nanoparticles for nose-to-brain delivery. Pharmaceutics. 2019;11(1):26.
- [29] Abonashey SG, Hassan H, Shalaby MA, Fouad AG, Mobarez E, El-Banna HA. Formulation, pharmacokinetics, and antibacterial activity of florfenicol-loaded niosome. Drug Delivery Transl Res. 2024:14:1077-92.
- [30] Li B, Shan M, Di X, Gong C, Zhang L, Wang Y, et al. A dual pH- and reduction-responsive anticancer drug delivery system based on PEG-SS-poly(amino acid) block copolymer. RSC Adv. 2017;7:30242-9.
- [31] Khalifa MM, Al-Karmalawy AA, Elkaeed EB, Nafie MS, Tantawy MA, Eissa IH, et al. Topo II inhibition and DNA intercalation by new phthalazine-based derivatives as potent anticancer agents: design, synthesis, anti-proliferative, docking, and in vivo studies. J Enzyme Inhib Med Chem. 2022;37:299-314.
- [32] Boraei ATA, Eltamany EH, Ali IAI, Gebriel SM, Nafie MS. Synthesis of new substituted pyridine derivatives as potent anti-liver cancer agents through apoptosis induction: In vitro, in vivo, and in silico integrated approaches. Bioorganic Chem. 2021;111:104877.
- Nafie MS, Elghazawy NH, Owf SM, Arafa K, Abdel-Rahman MA, **[331** Arafa RK. Control of ER-positive breast cancer by ERalpha expression inhibition, apoptosis induction, cell cycle arrest using semisynthetic isoeugenol derivatives. Chem Biol Interact. 2022;351:109753.
- Zhang J-Q, Li K, Cong Y-W, Pu S-P, Zhu H-Y, Xie X-G, et al. [34] Preparation, characterisation and bioactivity evaluation of the inclusion complex formed between picoplatin and y-cyclodextrin. Carbohydr Res. 2014;396:54-61.
- Dayyih AA, Gutberlet B, Preis E, Engelhardt KH, Amin MU, Abdelsalam AM, et al. Thermoresponsive liposomes for phototriggered release of hypericin cyclodextrin inclusion complex for efficient antimicrobial photodynamic therapy. ACS Appl Mater interfaces. 2022;14:31525-40.
- [36] Kurkov SV, Ukhatskaya EV, Loftsson T. Drug/cyclodextrin: beyond inclusion complexation. J Inclusion Phenom Macrocyclic Chem. 2011;69:297-301.
- [37] Fahmy SA, Ponte F, Abd El-Rahman MK, Russo N, Sicilia E, Shoeib T. Investigation of the host-quest complexation between 4-sulfocalix [4] arene and nedaplatin for potential use in drug delivery. Spectrochim Acta, Part A. 2018;193:528–36.
- [38] Praetorius A, Bailey DM, Schwarzlose T, Nau WM. Design of a fluorescent dye for indicator displacement from cucurbiturils: a macrocycle-responsive fluorescent switch operating through a pKa shift. Org Lett. 2008;10:4089-92.
- Wheate NJ, Abbott GM, Tate RJ, Clements CJ, Edrada-Ebel R, Johnston BF. Side-on binding of p-sulphonatocalix[4] arene to the dinuclear platinum complex trans-[{PtCl(NH3)2}2µ-dpzm]2 + and its implications for anticancer drug delivery. J Inorg Biochem. 2009;103:448-54.
- [40] Martinho N, Marques JMT, Todoriko I, Prieto M, de Almeida RFM, Silva LC. Effect of cisplatin and its catonic analogues in the phase behavior and permeability of model lipid bilayers. Mol Pharm. 2023;20:918-28.
- Justus CR, Dong L, Yang LV. Acidic tumor microenvironment and pH-sensing G protein-coupled receptors. Front Physiol. 2013:4:354.

18

- [42] Kato Y, Ozawa S, Miyamoto C, Maehata Y, Suzuki A, Maeda T, et al. Acidic extracellular microenvironment and cancer. Cancer Cell Int. 2013;13:89.
- [43] Kwon YJ, Seo EB, Jeong AJ, Lee SH, Noh KH, Lee S, et al. The acidic tumor microenvironment enhances PD-L1 expression via activation of STAT3 in MDA-MB-231 breast cancer cells. BMC Cancer. 2022:22:852.
- [44] Tang CH, Parham C, Shocron E, McMahon G, Patel N. Picoplatin overcomes resistance to cell toxicity in small-cell lung cancer cells previously treated with cisplatin and carboplatin. Cancer Chemother Pharmacol. 2011;67:1389–400.
- [45] Zhang D, Zhang J, Jiang K, Li K, Cong Y, Pu S, et al. Preparation, characterisation and antitumour activity of beta-, gamma- and HPbeta-cyclodextrin inclusion complexes of oxaliplatin. Spectrochim Acta A Mol Biomol Spectrosc. 2016;152:501–8.
- [46] Sokol MB, Chirkina MV, Yabbarov NG, Mollaeva MR, Podrugina TA, Pavlova AS, et al. Structural optimization of platinum drugs to improve the drug-loading and antitumor efficacy of PLGA nanoparticles. Pharmaceutics. 2022;14(11):2333.

- [47] Al Jayoush AR, Hassan HAFM, Asiri H, Jafar M, Saeed R, Harati R, et al. Niosomes for nose-to-brain delivery: A non-invasive versatile carrier system for drug delivery in neurodegenerative diseases.
  J Drug Delivery Sci Technol. 2023;89:105007.
- [48] Ma G, Kostevsek N, Monaco I, Ruiz A, Markelc B, Cheung CCL, et al. PD1 blockade potentiates the therapeutic efficacy of photothermally-activated and MRI-guided low temperaturesensitive magnetoliposomes. J Controlled Release. 2021;332:419–33.
- [49] Sedky NK, Mahdy NK, Abdel-kader NM, Abdelhady MMM, Maged M, Allam AL, et al. Facile sonochemically-assisted bioengineering of titanium dioxide nanoparticles and deciphering their potential in treating breast and lung cancers: biological, molecular, and computational-based investigations. RSC Adv. 2024;14:8583–601.
- [50] Ayoub AM, Amin MU, Ambreen G, Dayyih AA, Abdelsalam AM, Somaida A, et al. Photodynamic and antiangiogenic activities of parietin liposomes in triple negative breast cancer. Biomater Adv. 2022;134:112543.